Available online at www.sciencedirect.com

ScienceDirect

Advances in Space Research 57 (2016) 962–982

ADVANCES IN SPACE RESEARCH (a COSPAR publication)

www.elsevier.com/locate/asr

Developing the "Precessing Inclined Bi-Elliptical Four-Body Problem with Radiation Pressure" to search for orbits in the triple asteroid $2001SN_{263}$

Bruna Yukiko Pinheiro Lopes Masago [a], Antonio Fernando Bertachini de Almeida Prado [a,*], Ana Paula Marins Chiaradia [b], Vivian Martins Gomes [b]

[a] National Institute for Space Research, São José dos Campos, SP, Brazil
[b] São Paulo State University, FEG/UNESP, Guaratinguetá, SP, Brazil

Received 16 April 2015; received in revised form 26 November 2015; accepted 9 December 2015
Available online 17 December 2015

Abstract

Space missions to visit small bodies of the Solar System are important steps to improve our knowledge of the Solar System. Usually those bodies do not have well known characteristics, as their gravity field, which make the mission planning a difficult task. The present paper has the goal of studying orbits around the triple asteroid $2001SN_{263}$, a Near-Earth Asteroid (NEA). A mission to this system allows the exploration of three bodies in the same trip. The distances reached by the spacecraft from those three bodies have fundamental importance in the quality of their observations. Therefore, the present research has two main goals: (i) to develop a semi-analytical mathematical model, which is simple, but able to represent the main characteristics of that system; (ii) to use this model to find orbits for a spacecraft with the goal of remaining the maximum possible time near the three bodies of the system, without the need of space maneuvers. This model is called "Precessing Inclined Bi-Elliptical Problem with Radiation Pressure" (PIBEPRP). The use of this model allow us to find important natural orbits for the exploration of one, two or even the three bodies of the system. These trajectories can be used individually or combined in two or more parts using orbital maneuvers.
© 2015 COSPAR. Published by Elsevier Ltd. All rights reserved.

Keywords: Astrodynamics; Orbital maneuvers; Close approach trajectories; Small bodies

1. Introduction

Asteroids are celestial bodies orbiting the Sun which are too small to be considered planets. They receive different classifications, according to their orbital, physical, chemical and mineralogical characteristics. Most asteroids in the Solar System are located between the orbits of the planets Mars and Jupiter. This region is called as "main asteroid belt". Asteroids originated in that main belt and crossing the orbits of the terrestrial planets are called Near-Earth Asteroids (NEAs).

It is believed that most of the NEAs preserves information that could explain the formation of the Solar System, which is a point that indicates the importance to study them. In particular, it is believed that those objects hold information about the chemical mixture which formed the planets, as well as records of the geological evolution of the minor bodies in the interplanetary regions. Many missions have the goal of exploring these bodies, like Belton et al., 1992, 1996; Veverka et al., 2001; Yoshikawa et al., 2007; Jones et al., 2011; Huntress et al., 2006;

* Corresponding author.
E-mail addresses: brunamasago@gmail.com (B.Y.P.L. Masago), prado@dem.inpe.br (A.F.B.d.A. Prado), anachiaradia@feg.unesp.br (A.P.M. Chiaradia), vivianmartinsgomes@gmail.com (V.M. Gomes).

http://dx.doi.org/10.1016/j.asr.2015.12.007
0273-1177/© 2015 COSPAR. Published by Elsevier Ltd. All rights reserved.

Surovik and Scheeres, 2014; Broschart and Scheeres, 2005; Bellerose and Scheeres, 2008; Brum et al., 2011. Some other researches considered general trajectories around smaller bodies, which can be used in mission design of future missions to asteroids, like Werner, 1994; Rossi et al., 1999; Scheeres, 1994, 2012a–c; Scheeres and Hu, 2001; Bartczakk et al., 2006; Byram and Scheeres, 2009; Venditti and Prado, 2014.

The present research is related to the mission named ASTER, that has some preliminary studies available in the literature (Sukhanov et al., 2010; Macau et al. 2010). Its main objective is to study the triple NEA $2001SN_{263}$ (Araújo et al., 2012; Prado, 2014a, b), because it is believed that it contains information about the original composition of the Solar System.

Asteroids are bodies with small masses, so their gravity fields are weak. They also have irregular shaped bodies and the particular one studied here has two smaller bodies around it. The result of those facts is that orbits in this system are far from Keplerian. In that sense, predictions based in this simple model, usual when studying larger bodies, are not valid for more than a couple of hours, sometimes even less, depending on the geometry considered. So, in this way, the present paper has the goal of searching for orbits with the important property of allowing the spacecraft to spend the maximum possible time around one or more of the three bodies of the system, even if this observation time is not continuous and there is an alternation of periods when the spacecraft is not close to any of the bodies with periods of close approaches with them, without the need of orbital maneuvers. Solutions for this problem can be a single trajectory for the spacecraft. There is also the possibility to combine two or more trajectories shown here with orbital maneuvers, such that one trajectory can be used to observe one or two bodies and another solution to observe better the body that was not visible in details in the previous trajectories. It is also necessary to verify if those close approaches with the smaller bodies do not generate escaping trajectories, as a result of the energy gain generated by the close approaches involved (Broucke, 1988). The search for those types of orbits are particularly important if it is taken into account that orbits around the smaller primaries are hard to be found, because the masses of those bodies are too small.

To search for useful orbits, it was developed a semi-analytical mathematical model that takes into account all the important known features of this system of asteroids: the sizes and masses of the three bodies, the non spherical shape of the larger body and the effects of the radiation pressure. It is expected that the smaller two bodies are also not spherical, but their shapes are not known up to this point and for the larger body, only the J_2 term has an estimated value. Regarding the orbits of the smaller bodies, their semi-major axis, eccentricities and inclinations are known. In that sense, the "Precessing Inclined Bi-Elliptical Problem with Radiation Pressure (PIBEPRP)" is formulated here, where it is assumed that the origin of the reference system is the main body (Alpha) and that the reference plane is the orbital plane of the second largest body of the system, Beta. Both smaller bodies are assumed to be in elliptical orbits, with the smaller one (Gamma) in an inclined orbit with respect to the reference plane. The flattening of the main body is considered, both in terms of the effects caused directly in the trajectory of the spacecraft, as well as in terms of the indirect effects, since it generates a precession in the orbits of the two smaller bodies. This model is better explained later. Perturbations coming from outside the system are much smaller than the ones considered here, as shown by Prado (2014b), so this model is a good representation of the system. Tests including the Sun, the Moon and the planets Venus, Earth, Mars, Jupiter and Saturn were made with no significant differences in the results shown here. Another advantage of developing a model as the one presented here is that it can be used to study other similar systems, just by replacing the basic data and making a comparison of the perturbations received by the spacecraft in different positions. For asteroids far from the Sun and/or for missions using spacecrafts with small area/mass ratio, the version of the model without radiation pressure can be used, so the present model can be considered a special case of the restricted four body problem.

The results obtained using this model show that natural orbits useful to explore the three bodies are hard to find, but there are some options, although they do not last very long. There are also some solutions that can provide close encounters with one or two bodies of the system for a considerable amount of time, without generating escapes. It is also noticed that the effects of the radiation pressure depend on the trajectory under study, with respect to the time that the spacecraft remains near the three bodies. In some cases, it can even help to keep the spacecraft closer to the bodies longer, while in other situations it reduces the durations of the encounters. Some of the best trajectories use the radiation pressure to extend the duration of the encounters. There are also situations where the results are not modified by the presence of the radiation pressure.

2. The triple asteroid $2001SN_{263}$

The triple asteroid $2001SN_{263}$ is a Near-Earth Asteroid (NEA) discovered in 2008, by scientists from the Arecibo Observatory (Puerto Rico). They made several observations of this asteroid and found it was not just one body, but a triple system (Nolan et al., 2008). Two smaller bodies orbit the central asteroid (Alpha), so the whole system consists of Alpha, with 2.6 km in diameter, and two smaller bodies (Beta and Gamma), with 0.78 km and 0.58 km in diameter, respectively. The smaller bodies describe elliptical orbits around the larger one. Measured with respect to the central body, the second body has a semi-major axis of 16.633 km and an orbital period of 147 h. The third body has a semi-major axis of 3.804 km and an orbital period of 46 h (Becker et al., 2009).

Table 1
Physical and orbital components of the system $2001SN_{263}$ (Araújo et al., 2012).

Asteroid	Main body	a	e	i	Period	Radius	Mass
Alpha	Sun	1.99 AU	0.48	6.7°	2.80 years	1.3 km	917.47×10^{10} kg
Beta	Alpha	16.633 km	0.015	0.0°	6.23 days	0.39 km	24.04×10^{10} kg
Gamma	Alpha	3.804 km	0.016	13.87°	0.69 days	0.29 km	9.77×10^{10} kg

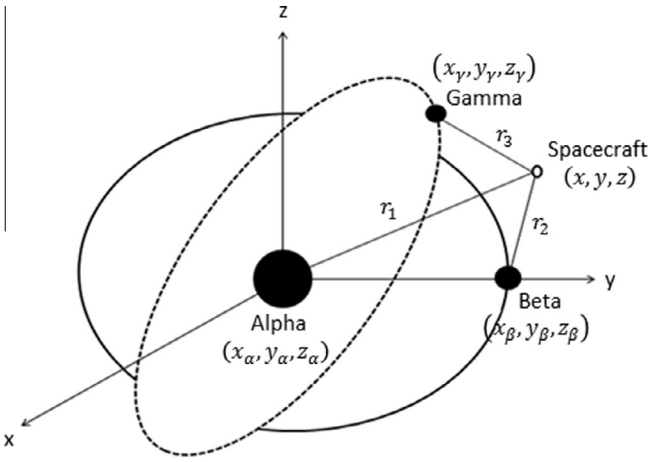

Fig. 1. Geometry of the system $2001SN_{263}$ (Masago, 2014).

The physical and orbital components of each body of the $2001SN_{263}$ system can be seen in Table 1, according to Araújo et al. (2012). The semi-major axis, eccentricity and inclination are represented, respectively, by the usual letters a, e, i. The term AU represents Astronomical Unit, that is the Sun-Earth distance.

3. The "Precessing Inclined Bi-Elliptical Problem with Radiation Pressure (PIBEPRP) model

As explained before, the first goal of the present research is to develop a semi-analytical mathematical model to study trajectories in the system $2001SN_{263}$ taking into account all the important known features of the asteroids. To build this model, it is assumed that the reference system is centered in the main body (Alpha) and the main reference plane is the orbital plane of Beta. Beta and Gamma are assumed to be in elliptical non-coplanar orbits. For the motion of the spacecraft, it is considered the gravitational forces of the three bodies, the flattening of the central body and the solar radiation pressure. The flattening of Alpha acts in both ways: directly in the trajectory of the spacecraft and indirectly, because it is considered that there is a precession in the orbits of the two smaller bodies due to this flattening. Fig. 1 shows the geometry of the problem.

In this figure $(x_\alpha, y_\alpha, z_\alpha)$ are the coordinates of Alpha, $(x_\beta, y_\beta, z_\beta)$ are the coordinates of Beta, $(x_\gamma, y_\gamma, z_\gamma)$ are the coordinates of Gamma and (x, y, z) are the coordinates of the spacecraft. Thus, r_1 is the distance between the spacecraft and Alpha; r_2 is the distance between the spacecraft and Beta; and r_3 is the distance between the spacecraft and Gamma, given by Eqs. (1)–(3)

$$r_1 = \sqrt{(x - x_\alpha)^2 + (y - y_\alpha)^2 + (z - z_\alpha)^2} \tag{1}$$

$$r_2 = \sqrt{(x - x_\beta)^2 + (y - y_\beta)^2 + (z - z_\beta)^2} \tag{2}$$

$$r_3 = \sqrt{(x - x_\gamma)^2 + (y - y_\gamma)^2 + (z - z_\gamma)^2} \tag{3}$$

These distances have to be monitored all the time, not only because they are required to evaluate the equations of motion, but also because the goal of this study is to find orbits that stay as long as possible near the three bodies. The equations of motion for the spacecraft in the inertial system, considering the above mentioned assumptions, are given by Eqs. (4)–(6), that are shown below

$$\ddot{x} = -\mu_\beta \frac{(x - x_\beta)}{r_1^3} - \mu_\gamma \frac{(x - x_\gamma)}{r_2^3} - \mu_\alpha \frac{(x - x_\alpha)}{r_3^3} - \mu_\alpha J_2 r_\alpha^2 \left(\frac{3x}{2r^5} - \frac{15z^2 x}{2r^7} \right) + P_{radx} \tag{4}$$

Table 2
Keplerian elements of Beta.

Semi-major axis (a_β)	16.633 km
Eccentricity (e_β)	0.015
Inclination (i_β)	0°
Ascending node (Ω_β)	0°
Argument of periapsis (ω_β)	$\omega_{0\beta} + \dot{\omega}_\beta t$ where $\omega_{0\beta} = 0$, $\dot{\omega}_\beta = 0.124°/\text{day} = 2.504870 \times 10^{-8}$ rad/s
Mean anomaly (M_β)	$M_\beta = n_\beta t$
n_β	$n_\beta = \left(\frac{\mu_\alpha}{a_\beta^3}\right)^{1/2} = 1.153566 \times 10^{-5}$ rad/s

Table 3
Keplerian elements for Gamma.

Semi-major axis (a_γ)	3.804 km
Eccentricity (e_γ)	0.016
Inclination (i_γ)	13.87° = 0.24rad
Ascending node (Ω_γ)	$\Omega_{0\gamma} + \dot{\Omega}_\gamma t$ where $\Omega_{0\gamma} = 0$, $\dot{\Omega}_\gamma = -1.338°/\text{day} = -2.702837 \times 10^{-7}$ rad/s
Argument of periapsis (ω)	$\omega_{0\gamma} + \dot{\omega}_\gamma t$ where $\omega_{0\gamma} = 0$, $\dot{\omega}_\gamma = 2.552°/\text{day} = 5.155185 \times 10^{-7}$ rad/s
Mean anomaly (M_γ)	$M_\gamma = n_\gamma t$
n_γ	$n_\gamma = \left(\frac{\mu_\alpha}{a_\gamma^3}\right)^{1/2} = 1.054721 \times 10^{-4}$ rad/s

Table 4
Orbit number, type of orbit and resonance, time (in days) that the spacecraft stays in a distance in the range 0–5 km from each body and the time (in days) that the spacecraft stays in a distance in the range 5–10 km from each body.

		Time in the given interval with no radiation pressure (days)		Time in the given interval with radiation pressure (days)			
				Anomaly = 0		Anomaly = 180°	
Orbit	*Orbits with the spacecraft starting in the periapsis (same side orbits)*	0–5 km	5–10 km	0–5 km	5–10 km	0–5 km	5–10 km
1	External orbit to Beta in resonance 5:2						
	R1	0	0	0	0	0	0
	R2	25.86	36.64	24.89	37.61	24.85	37.65
	R3	0	1.75	0	2.24	0	2.22
2	Internal orbit to Gamma in resonance 3:4						
	R1	51.65	10.85	33.24	7.95	46.09	6.43
	R2	0	0	0.26	1.59	0	0.26
	R3	23.61	38.89	23.47	17.56	31.19	20.48
3	Internal orbit to Gamma in resonance 4:5						
	R1	62.50	0	62.50	0	62.50	0
	R2	0	0	0	0	0	0
	R3	43.06	19.44	43.06	19.44	43.07	19.43
4	External orbit to Gamma in resonance 3:1						
	R1	19.74	35.69	29.00	25.50	6.99	16.70
	R2	0	3.43	0	0.52	0	1.70
	R3	21.26	28.32	23.04	27.69	5.70	15.56
	Orbits with the spacecraft starting in the apoapsis (same side orbits)						
5	Internal orbit to Beta in resonance 1:2						
	R1	0	0	0	0	0	0
	R2	62.50	0	62.50	0	62.50	0
	R3	0	0	0	0	0	0
6	Internal orbit to Beta in resonance 2:3						
	R1	0	0	0	0	0	0
	R2	62.50	0	62.50	0	62.50	0
	R3	0	0	0	0	0	0
7	Internal orbit to Beta in resonance 3:5						
	R1	0	0	0	0	0	0
	R2	62.50	0	62.50	0	62.50	0
	R3	0	0	0	0	0	0
8	Internal orbit to Beta in resonance 4:7						
	R1	0	0	0	0	0	0
	R2	62.50	0	62.50	0	62.50	0
	R3	0	0	0	0	0	0
9	Internal orbit to Beta in resonance 5:9						
	R1	0	0	0	0	0	0
	R2	62.50	0	62.50	0	62.50	0
	R3	0	0	0	0	0	0
10	External orbit to Gamma in resonance 2:1						
	R1	15.11	47.39	15.13	47.37	15.12	47.38
	R2	0	5.69	0	5.73	0	5.73
	R3	2.15	46.33	2.30	46.23	2.31	46.23
11	External orbit to Gamma in resonance 7:2						
	R1	0	0	0	0	0	0
	R2	62.50	0	62.50	0	62.50	0
	R3	0	0	0	0	0	0
12	External orbit to Gamma in resonance 4:3						
	R1	25.79	36.71	25.83	36.67	25.82	36.68
	R2	0	0.08	0	0	0	0
	R3	30.40	26.30	30.38	26.35	30.38	26.34

(*continued on next page*)

Table 4 (*continued*)

Orbit	*Orbits with the spacecraft starting in the apoapsis (same side orbits)*	Time in the given interval with no radiation pressure (days)		Time in the given interval with radiation pressure (days)			
				Anomaly = 0		Anomaly = 180°	
		0–5 km	5–10 km	0–5 km	5–10 km	0–5 km	5–10 km
13	External orbit to Gamma in resonance 7:3						
	R1	17.55	41.36	6.37	18.11	6.36	18.11
	R2	0	6.48	0	4.59	0	4.59
	R3	15.40	33.44	3.53	15.75	3.52	15.76
14	External orbit to Gamma in resonance 9:4						
	R1	20.88	40.56	8.74	28.26	8.75	28.30
	R2	0	5.42	0	4.91	0	4.91
	R3	14.61	35.38	3.11	24.66	3.10	24.66
15	External orbit to Gamma in resonance 7:5						
	R1	24.25	38.25	24.27	38.23	24.27	38.23
	R2	0	1.77	0	1.89	0	1.89
	R3	27.13	27.81	27.15	27.77	27.15	27.77
16	External orbit to Gamma in resonance 8:5						
	R1	56.75	5.75	5.53	2.16	5.53	2.16
	R2	0	0.16	0	0.16	0	0.16
	R3	22.36	39.88	4.18	3.25	4.17	3.25
	Orbits with the spacecraft starting in the periapsis (opposed orbits)						
17	Internal orbit to Gamma in resonance 4:5						
	R1	9.57	19.93	7.11	4.03	9.05	4.14
	R2	0	3.99	0	0.66	0	0.67
	R3	4.09	24.81	4.73	5.53	5.22	7.11
18	Internal orbit to Gamma in resonance 5:6						
	R1	9.65	2.25	51.11	11.39	11.84	6.29
	R2	0	0	0	0	0.50	3.20
	R3	5.26	6.29	17.39	45.11	8.39	9.92
19	External orbit to Gamma in resonance 2:1						
	R1	15.02	47.48	15.01	47.37	15.02	47.37
	R2	0	5.95	0	6.06	0	6.06
	R3	3.23	45.51	3.15	45.47	3.16	45.46
	Orbits with the spacecraft starting in the apoapsis (opposed orbits)						
20	External orbit to Gamma in resonance 6:5						
	R1	52.06	10.44	36.64	11.73	35.88	11.15
	R2	0	0	0.85	1.94	0.54	1.40
	R3	15.40	47.10	13.28	34.41	11.38	35.95
	Orbits with the spacecraft starting in the periapsis (same side orbits with i = 13, 87°)						
21	External orbit to Beta in resonance 5:2						
	R1	0	0	0	2.50	0	2.57
	R2	1.82	13.91	2.15	15.90	2.23	17.09
	R3	0	0.90	0	3.32	0.12	3.67
22	Internal orbit to Gamma in resonance 3:4						
	R1	62.50	0	62.50	0	62.50	0
	R2	0	0	0	0	0	0
	R3	42.96	19.54	43.03	19.47	43.03	19.47
23	Internal orbit to Gamma in resonance 4:5						
	R1	61.46	1.04	62.50	0	62.50	0
	R2	0	0	0	0	0	0
	R3	41.88	20.62	42.96	19.54	42.96	19.54
24	External orbit to Gamma in resonance 3:1						
	R1	1.27	2.91	0.52	1.35	0.53	1.35
	R2	0.80	2.09	0.76	1.32	0.77	1.32
	R3	1.51	3.08	0.99	0.72	1.00	0.73

(*continued on next page*)

Table 4 (*continued*)

Orbit	*Orbits with the spacecraft starting in the apoapsis (same side orbits with i = 13, 87°)*	Time in the given interval with no radiation pressure (days)		Time in the given interval with radiation pressure (days)			
				Anomaly = 0		Anomaly = 180°	
		0–5 km	5–10 km	0–5 km	5–10 km	0–5 km	5–10 km
25	Internal orbit to Beta in resonance 1:2						
	R1	2.34	16.04	4.50	17.21	3.18	14.24
	R2	1.38	11.07	0.88	6.42	1.59	5.57
	R3	2.99	16.60	3.39	17.44	2.70	13.11
26	Internal orbit to Beta in resonance 2:3						
	R1	0	0.89	0	0	0	0
	R2	24.42	32.49	14.04	21.90	13.30	18.96
	R3	0	2.70	0	0.94	0	0.94
27	Internal orbit to Beta in resonance 3:5						
	R1	2.25	16.76	1.51	10.37	6.58	20.79
	R2	2.80	10.19	6.02	11.68	4.57	9.27
	R3	3.45	15.08	1.24	9.88	5.82	19.11
28	Internal orbit to Beta in resonance 4:7						
	R1	0	1.66	0	1.65	0	1.65
	R2	1.60	1.17	1.59	1.18	1.59	1.18
	R3	0	2.33	0	2.28	0	2.29
29	Internal orbit to Beta in resonance 5:9						
	R1	0	1.59	0	1.56	0	1.56
	R2	2.06	1.61	2.00	1.66	2.01	1.66
	R3	0	2.06	0	2.00	0	2.00
30	External orbit to Gamma in resonance 2:1						
	R1	15.12	47.38	15.16	47.34	15.16	47.34
	R2	0	4.24	0	4.35	0	4.35
	R3	1.27	48.21	1.58	48.21	1.58	48.21
31	External orbit to Gamma in resonance 7:2						
	R1	11.79	31.83	5.95	20.77	5.28	22.69
	R2	0.66	3.84	5.84	10.18	1.40	3.41
	R3	12.38	25.19	4.90	21.46	7.87	14.46
32	External orbit to Gamma in resonance 4:3						
	R1	25.55	36.95	25.60	36.90	25.60	36.90
	R2	0	0.05	0	0.32	0	0.32
	R3	30.31	26.13	30.23	26.20	30.23	26.20
33	External orbit to Gamma in resonance 7:3						
	R1	7.40	25.17	19.25	28.72	9.21	32.10
	R2	3.12	9.69	0	3.87	0	8.55
	R3	4.50	22.49	15.54	24.81	8.16	27.32
34	External orbit to Gamma in resonance 9:4						
	R1	14.69	47.02	14.70	47.01	14.71	47.01
	R2	0	6.66	0	6.47	0	6.48
	R3	4.43	42.71	4.44	42.88	4.45	42.88
35	External orbit to Gamma in resonance 7:5						
	R1	24.44	38.06	24.56	37.94	24.56	37.94
	R2	0	0	0	0	0	0
	R3	26.82	28.54	27.17	28.28	27.17	28.28
36	External orbit to Gamma in resonance 8:5						
	R1	14.58	12.45	11.55	6.56	13.85	24.98
	R2	0	0.31	0	0.13	0	7.18
	R3	11.67	14.31	5.73	12.00	9.66	27.34

(*continued on next page*)

Table 4 (*continued*)

Orbit	*Orbits with the spacecraft starting in the periapsis (same side orbits with i = 90°)*	Time in the given interval with no radiation pressure (days)		Time in the given interval with radiation pressure (days)			
				Anomaly = 0		Anomaly = 180°	
		0–5 km	5–10 km	0–5 km	5–10 km	0–5 km	5–10 km
37	External orbit to Beta in resonance 5:2						
	R1	0	0	0	0	0	0
	R2	0	2.28	0	2.30	0	2.30
	R3	0	0	0	0	0	0
38	Internal orbit to Gamma in resonance 3:4						
	R1	8.13	8.68	8.13	8.69	8.13	8.67
	R2	0.38	0.67	0.34	0.73	0.38	0.66
	R3	4.42	11.87	4.42	11.76	4.42	11.90
39	Internal orbit to Gamma in resonance 4:5						
	R1	28.50	2.26	19.87	2.30	19.89	2.28
	R2	0	0	0	0	0	0
	R3	16.49	14.27	11.76	10.41	11.76	10.42
40	External orbit to Gamma in resonance 3:1						
	R1	2.39	4.46	3.31	6.08	2.61	4.84
	R2	0	0.46	0	0.47	0	0
	R3	1.54	4.62	2.16	6.35	1.45	4.77
	Orbits with the spacecraft starting in the apoapsis (same side orbits with i = 90°)						
41	Internal orbit to Beta in resonance 1:2						
	R1	3.56	7.09	3.80	7.41	3.79	7.40
	R2	0	0.57	0	0.58	0	0.58
	R3	3.10	6.39	3.10	6.99	3.27	6.62
42	Internal orbit to Beta in resonance 2:3						
	R1	2.50	10.09	2.17	9.57	2.17	9.60
	R2	0.65	3.21	0.34	3.42	0.34	3.44
	R3	1.46	10.50	0.88	10.53	1.01	10.48
43	Internal orbit to Beta in resonance 3:5						
	R1	3.66	12.52	3.31	11.47	3.31	11.47
	R2	0	1.78	0.19	2.06	0.19	2.06
	R3	3.17	10.73	3.21	9.57	3.21	9.57
44	Internal orbit to Beta in resonance 4:7						
	R1	2.13	8.66	2.36	8.90	2.36	8.90
	R2	0	2.01	0.15	1.85	0.16	1.84
	R3	2.64	7.17	2.58	7.77	2.48	7.54
45	Internal orbit to Beta in resonance 5:9						
	R1	3.49	15.01	2.89	13.99	2.89	14.00
	R2	0	1.18	0	1.35	0	1.36
	R3	4.62	12.13	3.29	11.57	3.50	11.34
46	External orbit to Gamma in resonance 2:1						
	R1	8.11	25.63	8.11	25.59	8.11	25.60
	R2	0	1.51	0	1.51	0	1.51
	R3	2.17	29.05	2.16	29.05	2.16	29.05
47	External orbit to Gamma in resonance 7:2						
	R1	3.12	5.93	3.16	5.99	3.71	6.84
	R2	0.22	0.88	0	1.24	0	0.57
	R3	2.56	5.68	2.58	5.46	2.89	7.16
48	External orbit to Gamma in resonance 4:3						
	R1	23.77	38.12	20.32	41.05	14.21	30.89
	R2	0	0	0	0.42	0.29	2.16
	R3	18.01	41.45	15.59	41.50	11.75	31.41

(*continued on next page*)

Table 4 (*continued*)

Orbit	*Orbits with the spacecraft starting in the apoapsis (same side orbits with i = 90°)*	Time in the given interval with no radiation pressure (days)		Time in the given interval with radiation pressure (days)			
				Anomaly = 0		Anomaly = 180°	
		0–5 km	5–10 km	0–5 km	5–10 km	0–5 km	5–10 km
49	External orbit to Gamma in resonance 7:3						
	R1	7.52	17.10	6.08	13.78	6.49	14.63
	R2	0	1.18	0	0.61	0	2.02
	R3	5.37	15.55	3.79	12.91	3.93	14.69
50	External orbit to Gamma in resonance 9:4						
	R1	8.47	21.85	8.40	21.68	8.25	21.49
	R2	0.32	1.79	0.21	2.04	0.46	1.91
	R3	4.65	23.24	4.64	22.21	4.90	22.02
51	External orbit to Gamma in resonance 7:5						
	R1	20.44	42.06	20.46	42.04	20.47	42.03
	R2	0	1.27	0	1.24	0	1.24
	R3	14.03	42.62	14.07	42.68	14.07	42.71
52	External orbit to Gamma in resonance 8:5						
	R1	18.24	39.68	11.13	25.92	9.94	23.00
	R2	0	2.60	0.41	1.51	0	1.44
	R3	13.47	39.70	10.07	24.69	8.13	21.79
	Orbits with the spacecraft starting in the periapsis (same side orbits with i = 180°)						
53	External orbit to Beta in resonance 5:2						
	R1	0	0	0	0	0	0
	R2	1.01	4.48	1.02	4.51	1.03	4.51
	R3	0	1.03	0	1.00	0	0.99
54	Internal orbit to Gamma in resonance 3:4						
	R1	4.24	0	4.24	0	4.24	0
	R2	0	0	0	0	0	0
	R3	2.13	2.11	2.14	2.11	2.13	2.11
55	Internal orbit to Gamma in resonance 4:5						
	R1	8.45	0	8.45	0	8.45	0
	R2	0	0	0	0	0	0
	R3	4.15	4.30	4.15	4.29	4.15	4.29
56	External orbit to Gamma in resonance 3:1						
	R1	1.95	3.89	1.95	3.90	1.95	3.90
	R2	0.53	1.82	0.53	1.82	0.53	1.82
	R3	1.64	4.64	1.65	4.62	1.65	4.63
	Orbits with the spacecraft starting in the apoapsis (same side orbits with i = 180°)						
57	Internal orbit to Beta in resonance 1:2						
	R1	1.14	2.32	2.31	7.68	1.14	2.32
	R2	0.37	1.69	0.66	2.94	0.37	1.68
	R3	0.80	2.92	1.61	8.49	0.80	2.92
58	Internal orbit to Beta in resonance 2:3						
	R1	0	0.92	0	0.92	0	0.92
	R2	0.15	0.55	0.15	0.55	0.15	0.55
	R3	0.11	0.68	0.11	0.68	0.11	0.68
59	Internal orbit to Beta in resonance 3:5						
	R1	1.57	13.17	1.88	10.64	1.87	10.64
	R2	3.14	7.11	2.68	6.89	2.68	6.89
	R3	2.92	11.29	2.61	10.02	2.61	10.05
60	Internal orbit to Beta in resonance 4:7						
	R1	1.19	2.96	2.05	9.56	1.65	4.06
	R2	0.48	2.89	1.62	5.19	1.06	3.54
	R3	0.94	3.40	2.31	9.26	1.35	4.51

(*continued on next page*)

Table 4 (*continued*)

Orbit	*Orbits with the spacecraft starting in the apoapsis (same side orbits with i = 180°)*	Time in the given interval with no radiation pressure (days)		Time in the given interval with radiation pressure (days)			
				Anomaly = 0		Anomaly = 180°	
		0–5 km	5–10 km	0–5 km	5–10 km	0–5 km	5–10 km
61	Internal orbit to Beta in resonance 5:9						
	R1	1.68	3.66	2.71	5.31	2.55	5.06
	R2	1.35	3.37	1.65	4.17	1.30	2.71
	R3	1.09	4.61	1.77	6.32	1.80	5.93
62	External orbit to Gamma in resonance 2:1						
	R1	14.22	48.28	14.35	48.15	14.34	48.16
	R2	0	4.29	0	4.15	0	4.14
	R3	13.10	33.88	13.42	34.29	13.43	34.28
63	External orbit to Gamma in resonance 7:2						
	R1	1.16	2.64	1.16	2.64	1.16	2.64
	R2	0.57	1.24	0.57	1.25	0.57	1.25
	R3	1.02	3.00	1.02	2.99	1.02	2.99
64	External orbit to Gamma in resonance 4:3						
	R1	7.50	7.29	7.47	7.33	7.47	7.32
	R2	0	0	0	0	0	0
	R3	5.71	9.08	5.71	9.08	5.71	9.09
65	External orbit to Gamma in resonance 7:3						
	R1	5.60	18.86	5.60	18.80	5.60	18.80
	R2	0	2.01	0	2.02	0	2.02
	R3	4.78	14.72	4.77	14.67	4.77	14.68
66	External orbit to Gamma in resonance 9:4						
	R1	4.60	14.33	4.61	14.29	4.61	14.29
	R2	0	2.49	0	2.49	0	2.49
	R3	3.93	12.25	3.91	12.25	3.91	12.25
67	External orbit to Gamma in resonance 7:5						
	R1	6.86	9.93	6.85	9.94	6.85	9.94
	R2	0	0	0	0	0	0
	R3	6.14	10.16	6.13	10.15	6.13	10.15
68	External orbit to Gamma in resonance 8:5						
	R1	11.26	20.08	11.25	20.08	11.24	20.08
	R2	0	0.24	0	0.26	0	0.26
	R3	10.76	18.39	10.75	18.30	10.75	18.30

$$\ddot{y} = -\mu_\beta \frac{(y-y_\beta)}{r_1^3} - \mu_\gamma \frac{(y-y_\gamma)}{r_2^3} - \mu_\alpha \frac{(y-y_\alpha)}{r_3^3} - \mu_\alpha J_2 r_\alpha^2 \left(\frac{3y}{2r^5} - \frac{15z^2 y}{2r^7}\right) + P_{rady} \quad (5)$$

$$\ddot{z} = -\mu_\beta \frac{(z-z_\beta)}{r_1^3} - \mu_\gamma \frac{(z-z_\gamma)}{r_2^3} - \mu_\alpha \frac{(z-z_\alpha)}{r_3^3} - \mu_\alpha J_2 r_\alpha^2 \left(\frac{9z}{2r^5} - \frac{15z^3}{2r^7}\right) + P_{radz} \quad (6)$$

where $J_2 = 0.013 \pm 0.008$ (Fang et al., 2011) is the constant that specifies the flattening of Alpha, $r = 1.3$ km is the radius of Alpha and P_{radx}, P_{rady}, P_{radz} represent the x, y and z components of the acceleration due to the solar radiation pressure. The gravitational parameters of the bodies Alpha, Beta and Gamma are given by $\mu_\alpha = m_\alpha G = 6.123458 \times 10^{-7}$ km^3 s^{-2}, $\mu_\beta = m_\beta G = 1.604499 \times 10^{-8}$ km^3 s^{-2} and $\mu_\gamma = m_\gamma G = 6.520778 \times 10^{-9}$ km^3 s^{-2}; where G is the universal gravitational constant, that is equal to 6.674287×10^{-20} km^3 kg^{-1} s^{-2}. The magnitude of the acceleration due to the radiation pressure is given by Eq. (7) shown below

$$P = \gamma \frac{h(1+\in)}{c} \frac{S}{m} \left(\frac{r_0}{R}\right)^2 \cos\alpha^2 \quad (7)$$

where S is the area of the spacecraft illuminated by the Sun; h is the solar radiation constant at the Sun–Earth distance (around 1360 [W/m^2]); r_0 is the Sun–Earth distance, R is the Sun–spacecraft distance, $\in$ is the coefficient of reflectivity; γ defines whether the spacecraft is in umbra ($\gamma = 0$), penumbra ($\gamma = 0.5$) or in an lighted region ($\gamma = 1.0$); and α is the angle of the incident light (Fieseler, 1988). The value used for S in all the simulations was 1 m^2 and the mass 100 kg, so S/m = 0.01 m^2/kg in all the results.

The coordinates of the bodies Beta and Gamma are obtained assuming that their orbits are ellipses that precess

due to the flattening of the main body (J_2). So, the argument of periapsis (ω) and the longitude of the ascending node (Ω) are functions of time. For the spacecraft, its motion is governed by the Keplerian gravitational forces of the three bodies, the flattening of Alpha and the radiation pressure coming from the Sun. Thus, this system is called "Precessing Inclined Bi-Elliptical Problem with Radiation Pressure", and has the acronym PIBEPRP associated with it. As previously stated, the PIBEPRP takes into account, in a relatively simple way, all the most relevant known features of this dynamical system. The only internal effects that are not considered are the effects of the gravitational forces of one smaller body in the other, but they are very small effects, due to the masses and distances involved. Prado (2014b) showed that external perturbations have effects with four orders of magnitude smaller than the internal forces, and are not important for the duration of the orbits studied here, that is of the order of two months. Numerical tests confirmed those assumptions.

To further develop the mathematical model, it is necessary to find how the Cartesian coordinates of the smaller bodies evolve with time, to make the numerical integrations of the equations of motion, as well as to monitor the distances between the spacecraft and the three bodies of the system. This information is the main criterion to choose the most suitable orbits. To perform this task, it is necessary to propagate the Keplerian elements taking into account the precession of the orbit and then make a coordinate transformation from the Keplerian elements of Beta and Gamma to their equivalent Cartesian elements at every instant of time. Several algorithms are available in the literature for those transformations, and the form used here is the one found in Kuga et al. (2012).

It is important to note that this transformation needs the eccentric anomaly of the smaller bodies. In the present research, this variable is obtained from the mean anomaly M using a Taylor series expansion of the Kepler's equation up to the third order, with the goal of obtaining a semi-analytical model. This expansion can be used here, because the eccentricities of both smaller bodies are of the order of 0.015, thus generating results with accuracy enough for our goals. Eq. (8) shows this relation

$$u = M + \left(e - \frac{1}{8}e^3\right)\sin M + \frac{1}{2}e^2 \sin 2M + \frac{3}{8}e^3 \sin 3M \qquad (8)$$

where u is the eccentric anomaly and e is the eccentricity of the orbit.

Therefore, the Keplerian elements of Beta are shown in Table 2. From those values it is possible to obtain the Cartesian elements of Beta at every instant of time, as explained before. The same steps are made for Gamma and its keplerian elements are shown in Table 3.

4. Results

The first point to be considered to obtain the results is how to choose the initial conditions for the orbits. The goal is to find orbits passing several times by the smaller bodies of the system, to compensate the fact that single orbits around those bodies do not last more than a few hours. In that way, orbits that are resonant with the orbits of the smaller bodies are good candidates to give initial conditions to generate trajectories with several passages by the smaller bodies. So, to simplify the calculations, the initial conditions of the spacecraft are obtained from points that belong to those resonant orbits. This is done for the Spacecraft-Beta and Spacecraft-Gamma systems, so it generates osculating orbits that are resonant with both of the smaller bodies. Next, these orbits are numerically integrated with the model shown before (PIBEPRP) and the results show the evolution of the distances between the spacecraft and the three bodies of the system, considering the three-dimensional space. The time the spacecraft stays inside a given range of distances is also important and com-

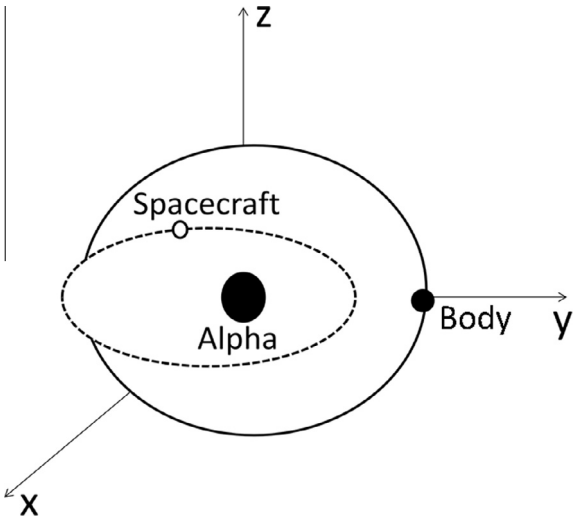

Fig. 2. Initial internal orbit (Masago, 2014).

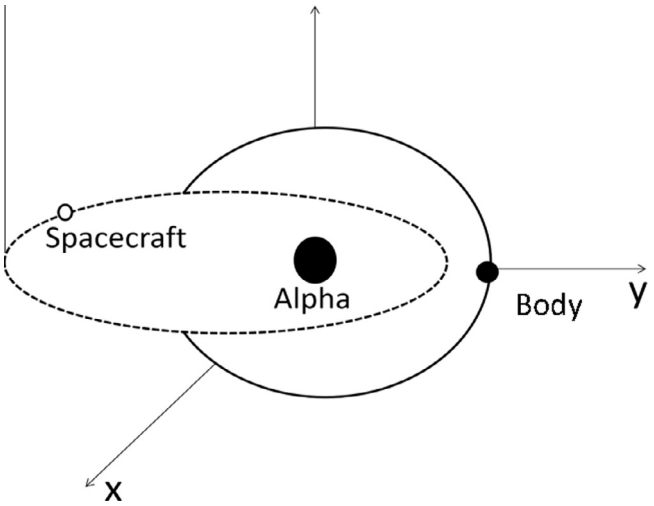

Fig. 3. Initial external orbit (Masago, 2014).

puted. Table 4 specifies the total time that the spacecraft stays in a given distance from the three bodies, allocated in two intervals: 0–5 km and 5–10 km. This is the most important criterion to choose the orbits. After that, the most interesting orbits are shown in more details. The asteroid has a very eccentric orbit (0.48), so three different situations are simulated: (i) with no radiation pressure effects, to represent situations where the area/mass ratio is very small, and also to identify explicitly the effects of this force; (ii) when the asteroid is at its periapsis (1 AU), so the effects of the radiation pressure reaches its maximum effects; (iii) when the asteroid is at its apoapsis (2 AU), so the effects of the radiation pressure is minimum.

Those families of orbits are identified and classified, generating a wide variety of options for the mission. It is important to note that the effects of the close approaches are taken into account when calculating the trajectories of the spacecraft, since the full dynamics is always considered in the evolution of the orbits. It means that the orbits that make the spacecraft to escape from the system are identified and can be avoided.

Figs. 2 and 3 show how to obtain the resonant condition. It is necessary to consider the problem as divided in two cases: initial internal orbits, shown in Fig. 2, that means that the semi-major axis of the spacecraft is smaller than the semi-major axis of the body considered; or initial external orbits, shown in Fig. 3, where the semi-major axis of the spacecraft is larger than the semi-major axis of the orbit of the body considered. Both situations are considered in the present research.

This division is necessary for the correct use of the terms in the equation that expresses the resonant condition. For the internal orbits it is used Eq. (9) (Murray and Dermott, 1999).

$$\frac{n' - \dot{\varpi}'}{n - \dot{\varpi}'} = \frac{p}{p+q} = \frac{n'}{n} \tag{9}$$

where n is the mean motion of the spacecraft, n' is the mean motion of Beta or Gamma, $\dot{\varpi}'$ is the time variation of the longitude of the periapsis of Beta or Gamma. The order of the resonance is given by p and q, where p is the number of revolutions of the body considered (Beta or Gamma) and $(p+q)$ is the number of revolutions of the spacecraft. The calculation of the external initial orbits is based in Eq. (10) shown below (Murray and Dermott, 1999):

$$\frac{n' - \dot{\varpi}'}{n - \dot{\varpi}'} = \frac{p+q}{p} = \frac{n'}{n} \tag{10}$$

where n is now the mean motion of Beta or Gamma, n' is now the value of the mean motion of the spacecraft, $\dot{\varpi}'$ is still the time derivative of the longitude of the periapsis of Beta or Gamma. The order of the resonance is again given by p and q, where p is now the number of revolutions of the spacecraft and $(p+q)$ is now the number of revolutions of the body considered (Beta or Gamma).

The values used for p and q are in the interval 1–5. Larger values generate orbits with very long periods, which have little practical interest, since the duration of the mission would be too large to get a good number of close encounters with Beta and Gamma.

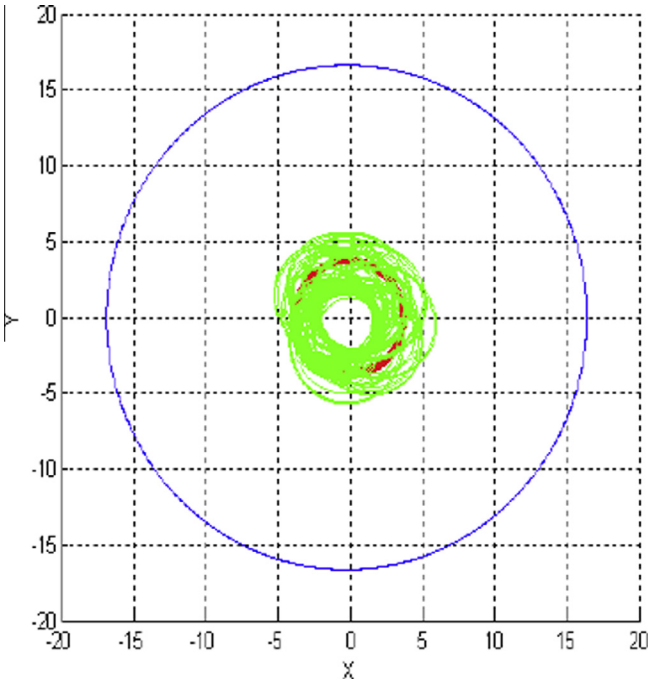

Fig. 4a. Trajectory of the spacecraft (green), Beta (blue) and Gamma (red) when there is no radiation pressure for orbit 2, in km. (For interpretation of the references to color in this figure legend, the reader is referred to the web version of this article.)

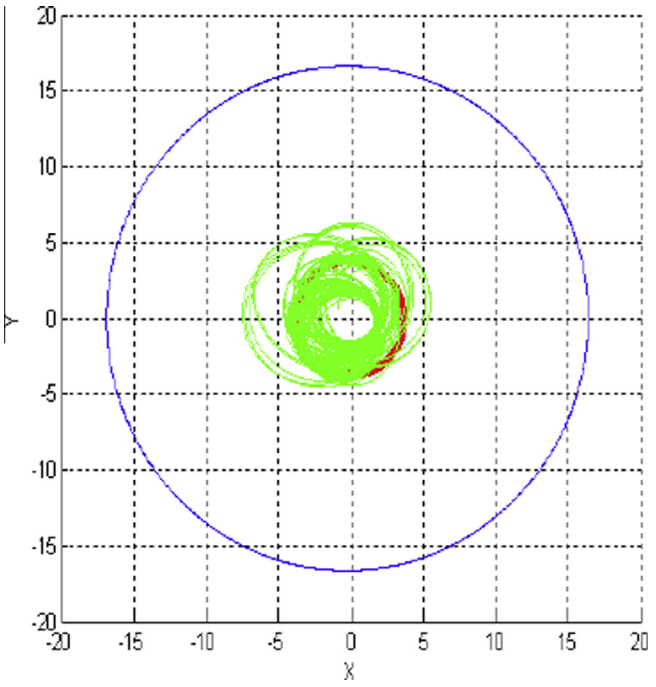

Fig. 4b. Trajectory of the spacecraft (green), Beta (blue) and Gamma (red) when there is radiation pressure and the asteroid is at the apoapsis for orbit 2, in km. (For interpretation of the references to color in this figure legend, the reader is referred to the web version of this article.)

A first analysis was performed by looking at the eccentricities obtained for the orbits. The ones that have eccentricities larger than 1.0 were discarded, because they are hyperbolic orbits, therefore they do not allow repeated encounters between the spacecraft and the secondary bodies. A second analysis is made by calculating the radius of the periapsis. If $r_p < 2$ km, the orbit will be also eliminated due to the high risk of collision with the central body.

Next, a detailed analysis is made, using plots indicating the distances between Alpha and the spacecraft (r_1), Beta and the spacecraft (r_2), and Gamma and the spacecraft (r_3). Those plots are made as a function of time, to verify the effects of the bodies Beta and Gamma in the orbit of the spacecraft, in the particular point of the evolution of these distances. The total time the spacecraft stays near each of the three bodies are computed and presented in Table 4 for the three situations already mentioned: no effects of the radiation pressure and including the radiation pressure with the asteroid at the apoapsis and the periapsis of its trajectory around the Sun.

Once the resonant orbits that intersect with at least one of the orbits of the smaller bodies and do not collide with any of them are found, these trajectories are numerically integrated using the dynamical model given by the PIBEPRP. The duration of the integration is not always the same, since most orbits show a risk of collision with one of the bodies of the system. These orbits are not discarded, because the collisions can be avoided by orbital maneuvers, but the numerical integrations are stopped at this point. Two different situations are used for the initial position: with the spacecraft starting at the periapsis or at the apoapsis of its initial orbit. Two geometries are also considered for the relative positions of the two satellite bodies: with both of them in the same side with respect

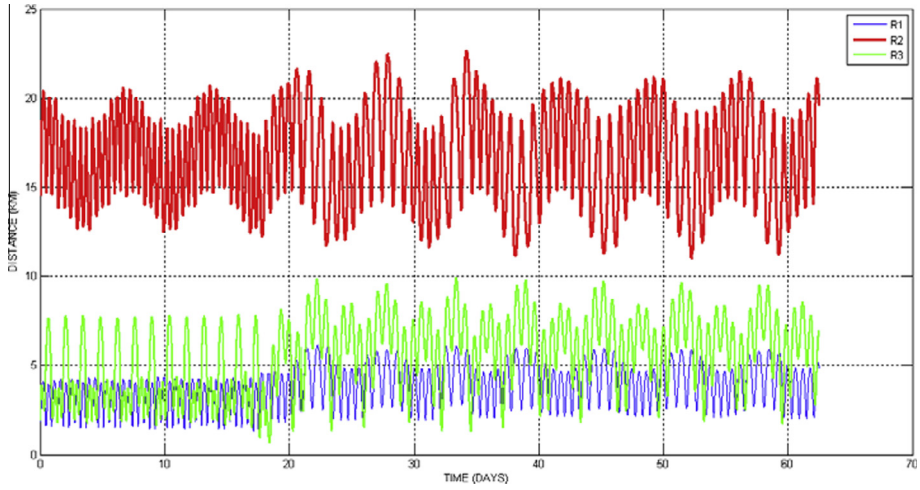

Fig. 4c. Distances of the spacecraft as a function of time from Alpha (blue), Beta (red) and Gamma (green) when there is no radiation pressure for orbit 2. (For interpretation of the references to color in this figure legend, the reader is referred to the web version of this article.)

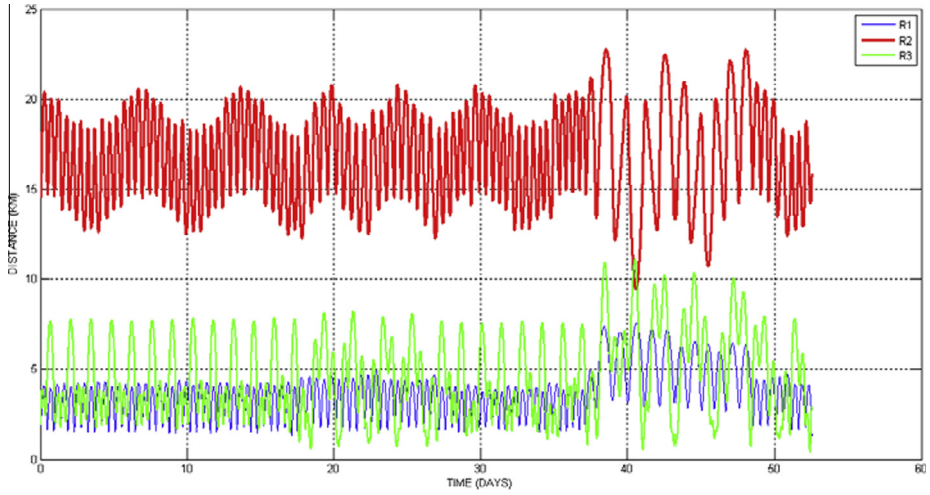

Fig. 4d. Distances of the spacecraft as a function of time from Alpha (blue), Beta (red) and Gamma (green) when there is radiation pressure and the asteroid is at the apoapsis for orbit 2. (For interpretation of the references to color in this figure legend, the reader is referred to the web version of this article.)

to the central body (this geometry is called "same side geometry") and when they are in opposite directions with respect to the central body (that is called "opposite geometry"). Table 4 shows all the results, describing the identification number of the orbit, the type of the orbit and resonance, the time (in days) that the spacecraft stays in a distance in the range of 0–5 km from each body and the time (in days) the spacecraft stays in a distance in the range of 5–10 km from each body. There are six columns to express those results. The first two of them consider the case with no radiation pressure effects; the third and the fourth columns represent the cases where the asteroid is at the periapsis; and the last two columns are for the situation with the asteroid at the apoapsis. Four different inclinations are considered for the initial orbit of the spacecraft: 0° (a direct orbit in the orbital plane of Beta), 13.87° (a direct orbit in the orbital plane of Gamma), 90° (an orbit perpendicular to the orbital plane of Beta), and 180° (a retrograde orbit in the orbital plane of Beta). Only the more interesting solutions are shown in Table 4, to avoid a large number of data with very little practical interest. The results show the existence of several types of orbits, that are described below.

(1) Orbits that escaped very fast from the system due to a close approach with one of the secondary bodies, which are usually omitted here, except for one example (orbit 37).

(2) Orbits that escaped from the system or collided with one of the bodies, but survived for a few days. Those orbits are listed in Table 4, because they can be used

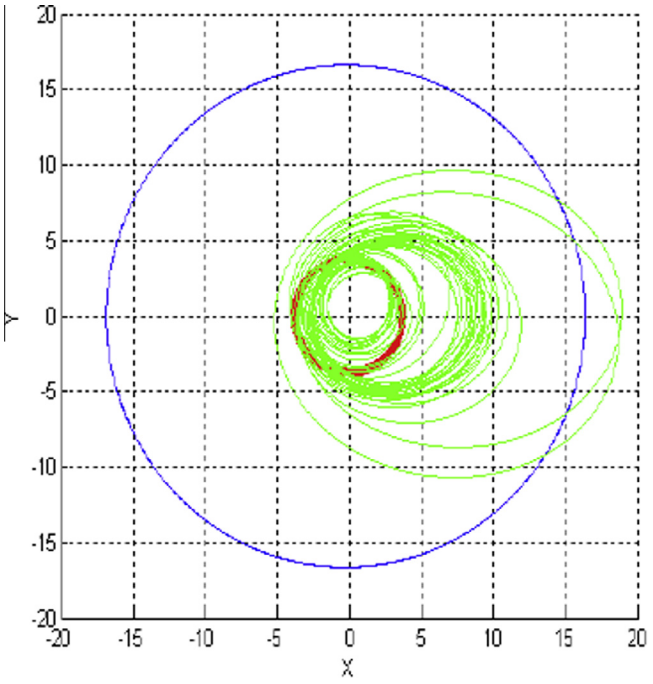

Fig. 5b. Trajectory of the spacecraft (green), Beta (blue) and Gamma (red) when there is radiation pressure and the asteroid is at the periapsis for orbit 33, in km. (For interpretation of the references to color in this figure legend, the reader is referred to the web version of this article.)

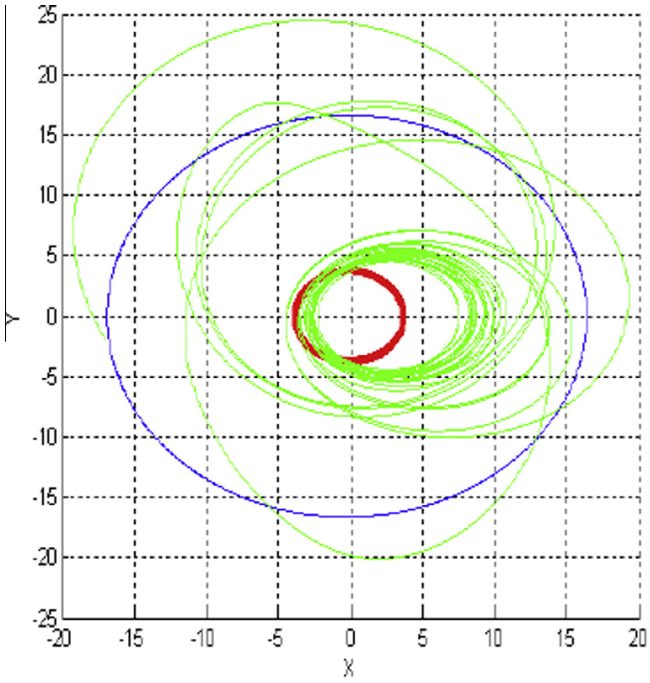

Fig. 5a. Trajectory of the spacecraft (green), Beta (blue) and Gamma (red) when there is no radiation pressure for orbit 33, in km. (For interpretation of the references to color in this figure legend, the reader is referred to the web version of this article.)

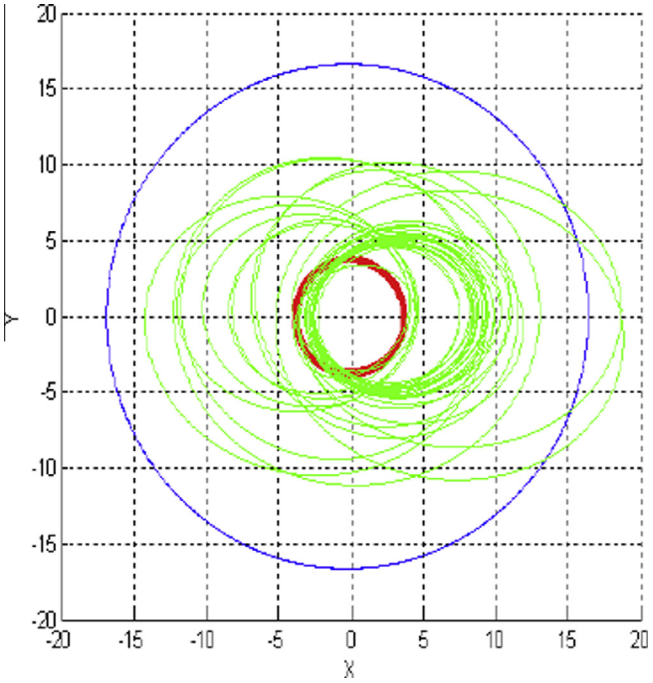

Fig. 5c. Trajectory of the spacecraft (green), Beta (blue) and Gamma (red) when there is radiation pressure and the asteroid is at the apoapsis for orbit 33, in km. (For interpretation of the references to color in this figure legend, the reader is referred to the web version of this article.)

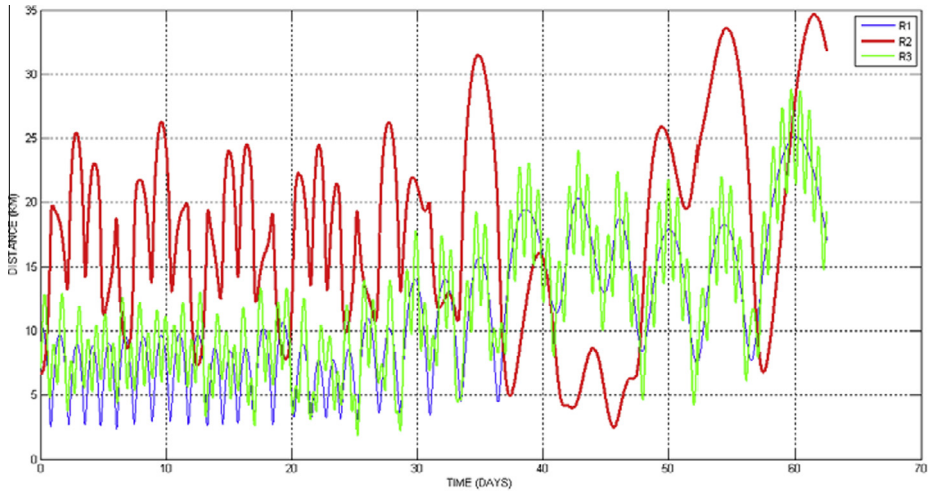

Fig. 5d. Distances of the spacecraft as a function of time from Alpha (blue), Beta (red) and Gamma (green) when there is no radiation pressure for orbit 33. (For interpretation of the references to color in this figure legend, the reader is referred to the web version of this article.)

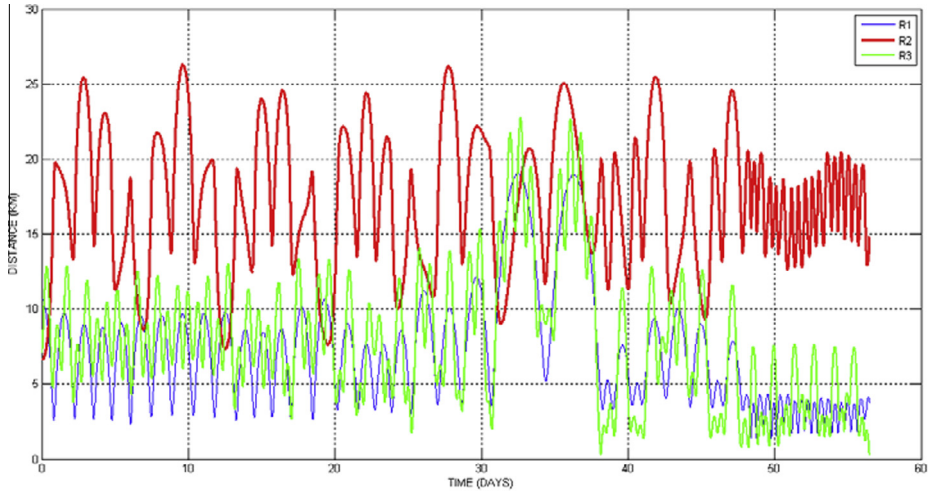

Fig. 5e. Distances of the spacecraft as a function of time from Alpha (blue), Beta (red) and Gamma (green) when there is radiation pressure and the asteroid is at the periapsis for orbit 33. (For interpretation of the references to color in this figure legend, the reader is referred to the web version of this article.)

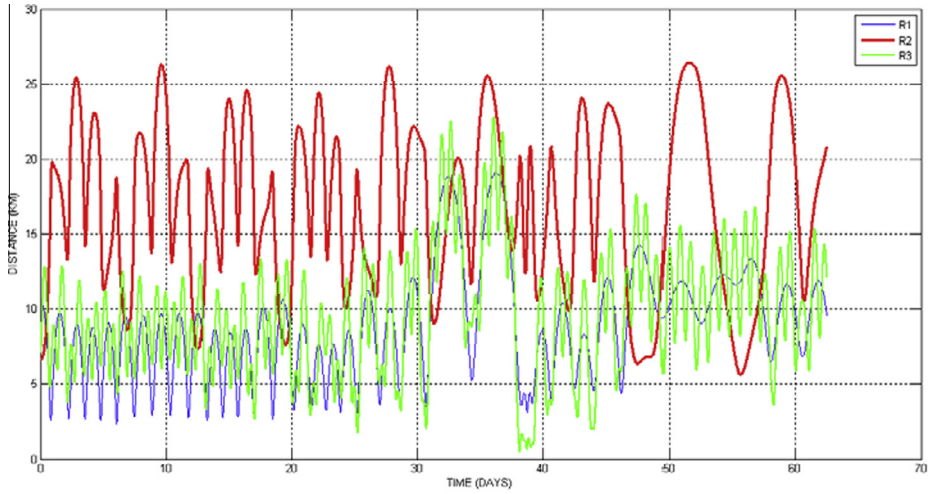

Fig. 5f. Distances of the spacecraft as a function of time from Alpha (blue), Beta (red) and Gamma (green) when there is radiation pressure and the asteroid is at the apoapsis for orbit 33. (For interpretation of the references to color in this figure legend, the reader is referred to the web version of this article.)

as part of a more complex trajectory that has some maneuvers to link two or more of the orbits found here.

(3) Orbits that are excellent to observe the bodies Alpha and Gamma. Those bodies are close to each other, so there are many single natural orbits that spend a long time around both of them.

(4) Orbits that stay around the body Beta, allowing a long time to observe it.

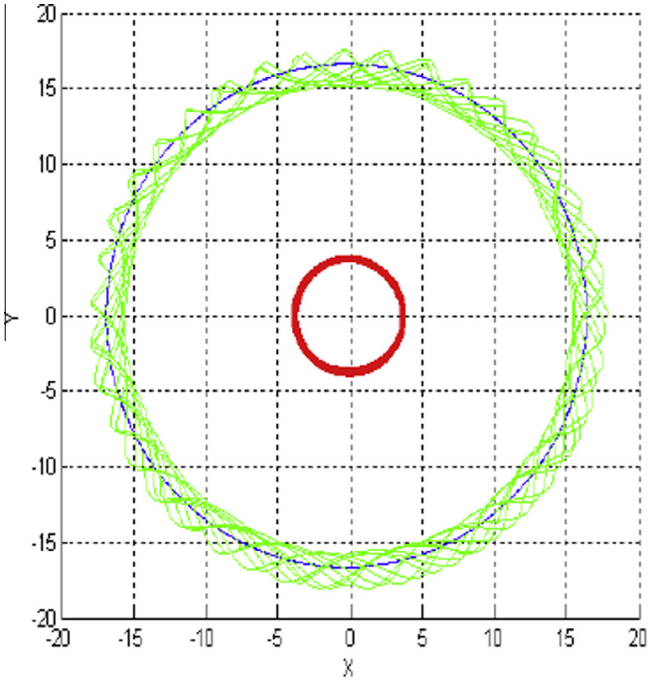

Fig. 6a. Trajectory of the spacecraft (green), Beta (blue) and Gamma (red) when there is radiation pressure and the asteroid is at the periapsis for orbit 5, in km. (For interpretation of the references to color in this figure legend, the reader is referred to the web version of this article.)

(5) Orbits that have passages by the three bodies, which can be used to observe all of them in a single natural trajectory. There are a few orbits with this property, and the durations of the encounters are not very long, but they are interesting options to be considered by mission designers, if orbital maneuvers can be used to start again a new cycle.

In general, it is interesting to see that the trajectories starting with inclinations different from zero (polar or in the plane of the orbit of Gamma and retrograde) stay always near one of the bodies until a collision or an escape occurs. Note that there are only zeros in the time the spacecraft stays in the range from 5 to 10 km.

The effects of the radiation pressure can be analyzed in details from those results. Regarding the time the spacecraft remain closer to the asteroids, which are the focus of the present research, there are three different situations: (i) orbits which results are not affected by the radiation pressure, because they are close to the bodies and the gravity forces dominate the motion of the spacecraft; (ii) orbits where the spacecraft remains less time near the asteroids, so giving less interesting results, in particular strongly reducing the time the spacecraft remains at a distance from 5 to 10 km from the bodies; (iii) orbits with the spacecraft spending more time near the bodies, so helping the observation of the asteroids.

4.1. Orbits to observe Alpha and Gamma

The first family of results describes orbits for the spacecraft that are suitable to observe the bodies Alpha and Gamma. All types of orbits are considered, with initial conditions in resonant orbits with Beta or Gamma; internal and external orbits; with the spacecraft leaving from the periapsis or apoapsis. From Table 4 it is possible to have

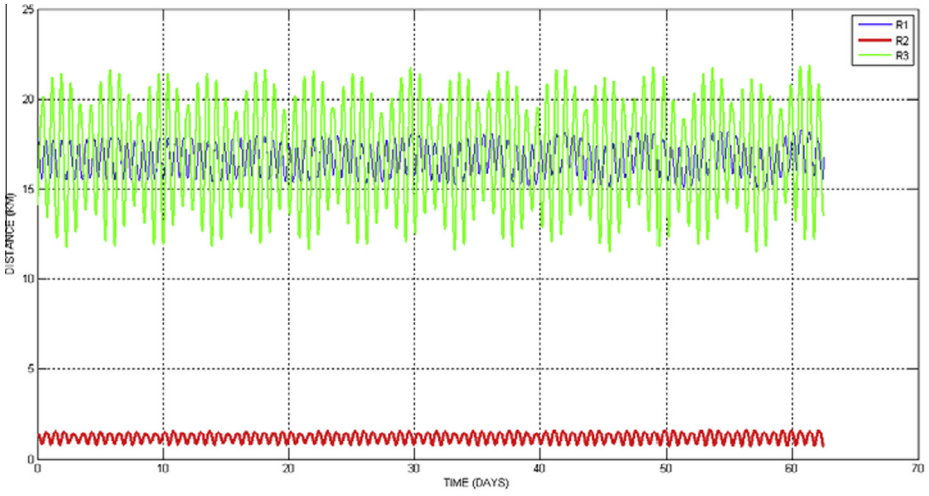

Fig. 6b. Distances of the spacecraft as a function of time from Alpha (blue), Beta (red) and Gamma (green) when there is radiation pressure and the asteroid is at the apoapsis for orbit 5. (For interpretation of the references to color in this figure legend, the reader is referred to the web version of this article.)

a general view and the mission designers can choose orbits from there. There are many options where the spacecraft stays a long time passing by Alpha and Gamma. Some of the more interesting orbits are described in detail in the next figures. The fact that Alpha and Gamma are close to each other helps to find a large number of solutions to study those two bodies in a single natural trajectory. It is noted that the durations of the trajectories are not the same. Some trajectories, as 22, survived for the whole integration time, that is 62.5 days in each simulation. In particular, this orbit keeps the spacecraft near Alpha all the time and close to Gamma about 70% of the time, so it is a very interesting trajectory to study those two bodies. This orbit has little effects from the radiation pressure, because it passes near the two bodies, so their gravity field dominates the motion of the spacecraft. There is only a slight increase in the time the spacecraft spends near Gamma. As an example of the technique used in the present paper,

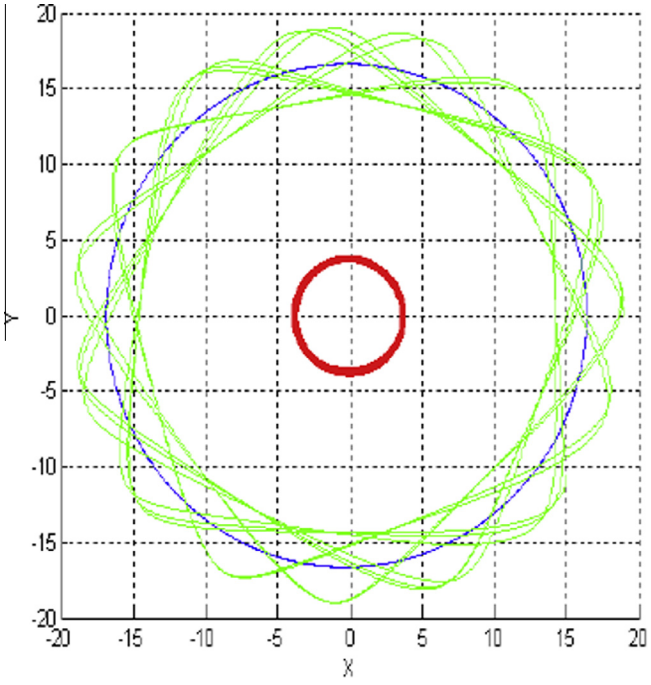

Fig. 7a. Trajectory of the spacecraft (green), Beta (blue) and Gamma (red) when there is radiation pressure and the asteroid is at the periapsis for orbit 7. (For interpretation of the references to color in this figure legend, the reader is referred to the web version of this article.)

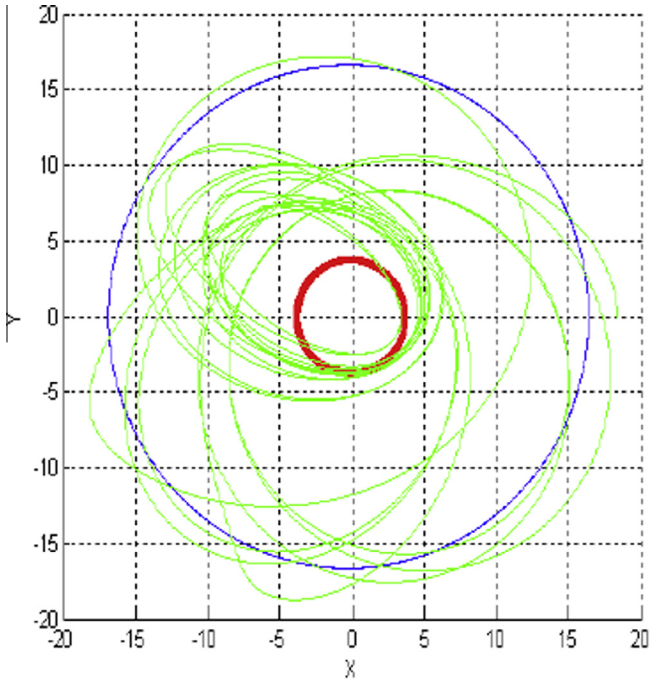

Fig. 8a. Trajectory of the spacecraft (green), Beta (blue) and Gamma (red) when there is no radiation pressure for orbit 27, in km. (For interpretation of the references to color in this figure legend, the reader is referred to the web version of this article.)

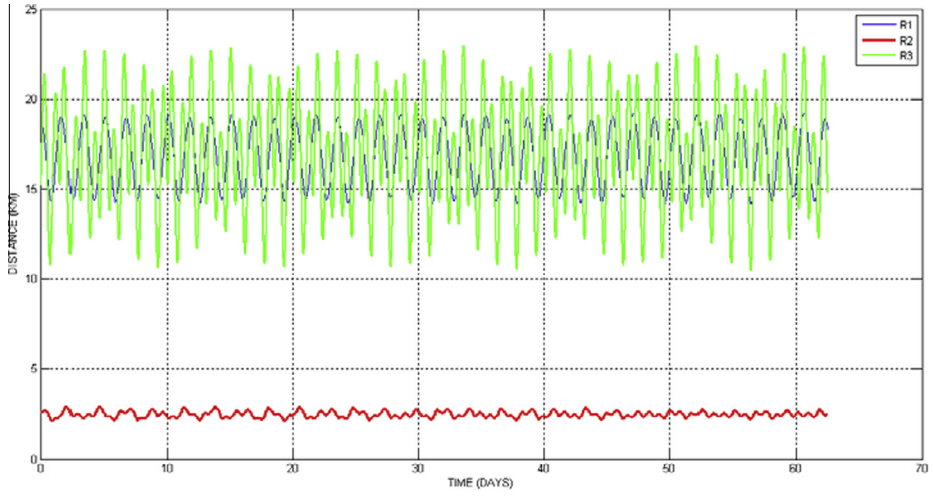

Fig. 7b. Distances of the spacecraft as a function of time from Alpha (blue), Beta (red) and Gamma (green) when there is radiation pressure and the asteroid is at the apoapsis for orbit 7. (For interpretation of the references to color in this figure legend, the reader is referred to the web version of this article.)

Figs. 4a and c show the trajectories and the distances between the spacecraft and the three bodies of the system, as a function of time, for orbit number 2, that is an internal orbit starting at the 3:4 resonance with Gamma. This is a very interesting trajectory. When the radiation pressure is not considered, so assuming a spacecraft with low ratio area/mass, this trajectory allows the spacecraft to stay 51.65 days near Alpha and 23.61 days near Gamma, from 62.5 simulated days. If the radiation pressure is considered and the asteroid is at the periapsis of its trajectory around the Sun the durations of the encounters are modified to 33.24 days near Alpha and 23.47 days near Gamma, that is still a very good result. If the asteroid is at the apoapsis of its trajectory around the Sun, those durations are modified to 46.09 days near Alpha and 31.19 days near Gamma, that is even a much better result to observe both bodies, with the durations better distributed between the two bodies. Figs. 4b and d show the trajectories with radiation pressure and with the radiation pressure when the asteroid at the apoapsis, as well as the evolution of the distances from the three bodies as a function of time.

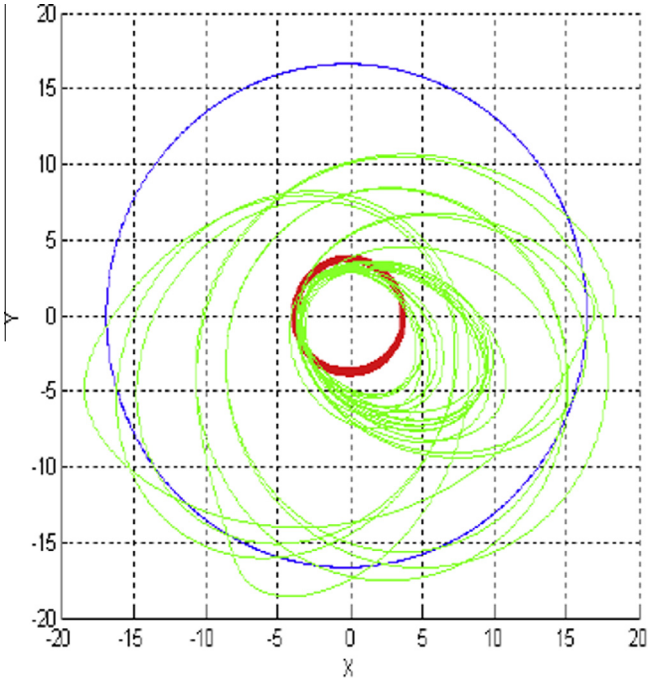

Fig. 8b. Trajectory of the spacecraft (green), Beta (blue) and Gamma (red) when there is radiation pressure and the asteroid is at the apoapsis for orbit 27, in km. (For interpretation of the references to color in this figure legend, the reader is referred to the web version of this article.)

Table 4 shows also that orbit number 4 is another example of trajectory that benefits from the radiation pressure to stay longer near the bodies Alpha and Gamma. The time increases from 19.74 days near Alpha, when there is no radiation pressure, to 29.00 days when the radiation pressure is considered and the asteroid is at the periapsis. Regarding Gamma, the observation time goes from 21.26 days to 23.04 days.

Another very interesting trajectory is orbit number 18. It is noted that, when the radiation pressure is not considered, the spacecraft stays 9.65 days near Alpha and 5.26 days near Gamma. These shorter durations of the encounters are due to a collision with Gamma. When adding the radiation pressure and the asteroid is at the periapsis, this collision no longer occurs, and the spacecraft stays 51.11 days near Alpha and 17.39 days near Gamma. This is a situation where the radiation pressure helped the spacecraft to stay much more longer near the asteroids. It is one of the best trajectories found here, thanks to the presence of the radiation pressure.

Fig. 5 shows orbit number 33, that is an external orbit starting at the 7:3 resonance with Gamma. This is also an interesting trajectory. When the radiation pressure is not considered, this trajectory has short passages, but the spacecraft passes by the three bodies. The spacecraft stays 7.40 days near Alpha, 3.12 days near Beta and 4.50 days

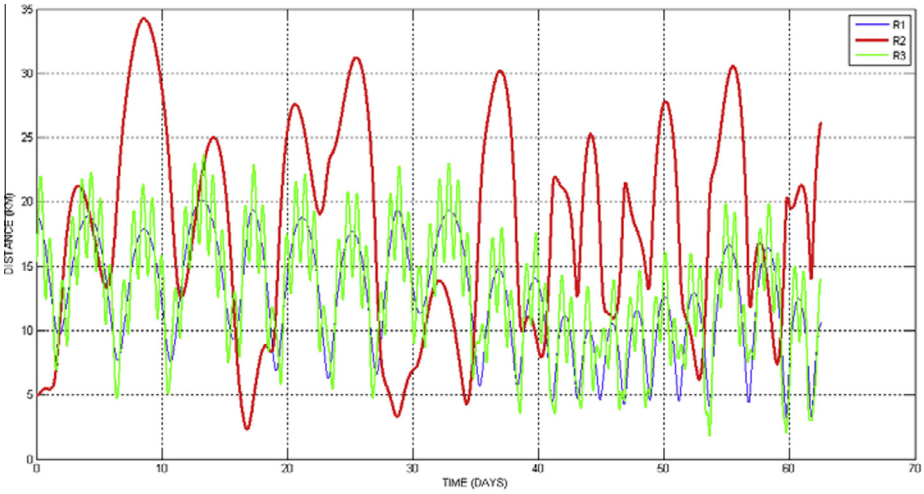

Fig. 8c. Distances of the spacecraft as a function of time from Alpha (blue), Beta (red) and Gamma (green) when there is no radiation pressure for orbit 27. (For interpretation of the references to color in this figure legend, the reader is referred to the web version of this article.)

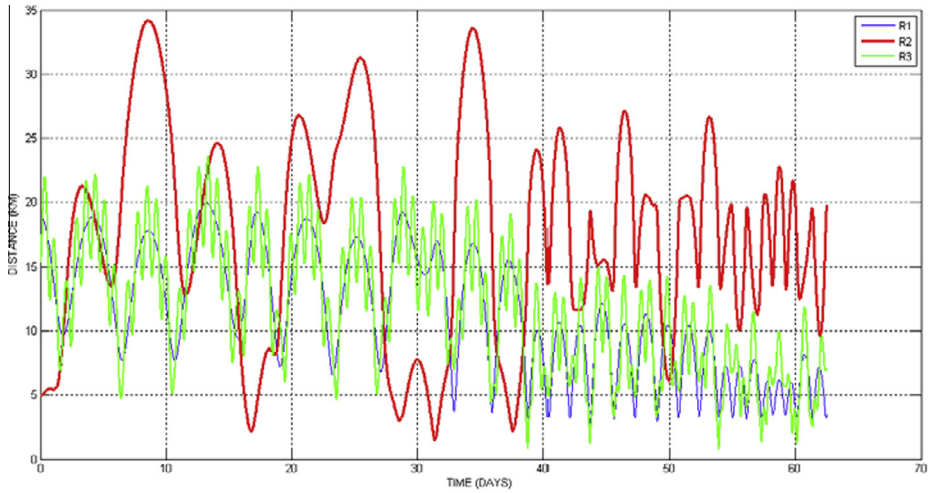

Fig. 8d. Distances of the spacecraft as a function of time from Alpha (blue), Beta (red) and Gamma (green) when there is radiation pressure and the asteroid is at the apoapsis for orbit 27. (For interpretation of the references to color in this figure legend, the reader is referred to the web version of this article.)

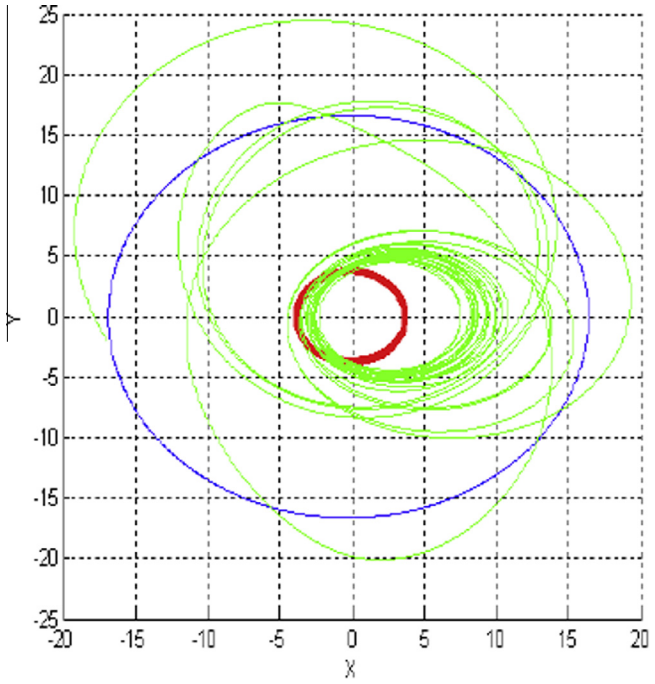

Fig. 9a. Trajectory of the spacecraft (green), Beta (blue) and Gamma (red) when there is no radiation pressure for orbit 31. (For interpretation of the references to color in this figure legend, the reader is referred to the web version of this article.)

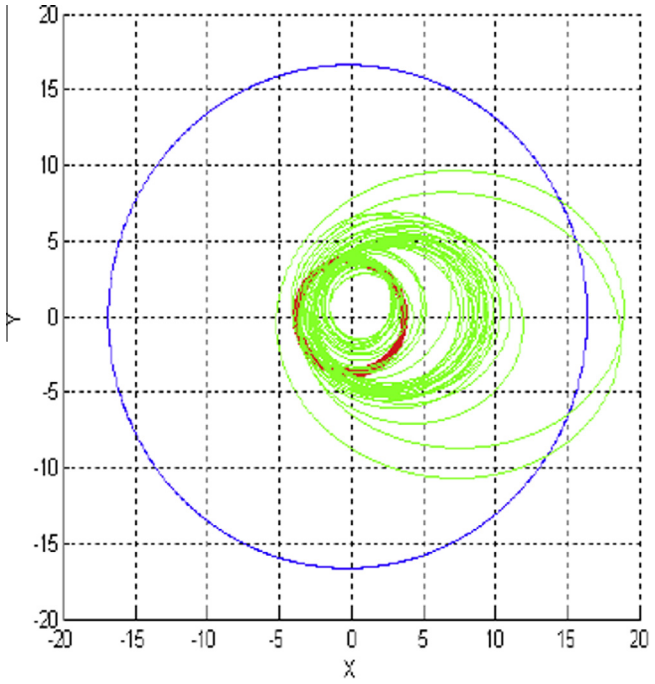

Fig. 9b. Trajectory of the spacecraft (green), Beta (blue) and Gamma (red) when there is radiation pressure and the asteroid is at the periapsis for orbit 31. (For interpretation of the references to color in this figure legend, the reader is referred to the web version of this article.)

near Gamma. If the radiation pressure is considered and the asteroid is at the periapsis of its trajectory around the Sun, those times are modified. There is no close approach to Beta, but the time near the other two bodies increases to 19.25 days near Alpha and 15.54 days near Gamma. So, it is now a good trajectory to observe Alpha and Gamma. The radiation pressure had a strong effect in this trajectory.

4.2. Orbits to observe Beta

The second family of trajectories describes orbits for the spacecraft that allows the observation of the body Beta. In most of the cases the spacecraft is captured by Beta. Thus, those orbits are only interesting to explore this body. Once again, all combinations of initial conditions are considered: initial orbits resonant with Beta and Gamma and internal

and external orbits. The same two situations, where the spacecraft leaves from the periapsis and apoapsis of its orbit, are considered. Table 4 shows several options. Similarly to what happened in the previous case, the durations of the trajectories are not the same. Some trajectories, as numbers 5 and 7, lasted the whole integration time of 62.5 days. Figs. 6a and b show trajectories and distances for the orbit number 5 and Figs. 7a and b show the same results for orbit number 7. The radiation pressure has minimum effects on those two trajectories, because the spacecraft remains all the time close to Beta and its gravitational field dominates the motion of the spacecraft.

4.3. Orbits to observe the three bodies

The third family of results describes orbits for the spacecraft that allow the observation of the three bodies of the system in a single trajectory. In the majority of the cases, the spacecraft does not stay longer near each body. Thus, those orbits are only interesting whether short times are enough to observe the bodies or whether maneuvers can be made to start the same or a similar cycle again. As done before, initial orbits resonant with Beta and Gamma and internal and external orbits are considered, as well as the situations where the spacecraft leaves from the periapsis and apoapsis of its orbit. Table 4 shows the existence of several useful trajectories to observe the three bodies in a single natural trajectory.

Some trajectories, as 24, lasted less than 12 days. Two good examples of useful trajectories to observe all the bodies are shown in detail in Figs. 8 and 9. Orbit number 27 is shown in Fig. 8, that is an internal orbit in resonance 3:5 with Beta. It is another example of trajectory that benefits from the effects of the solar radiation pressure. When the

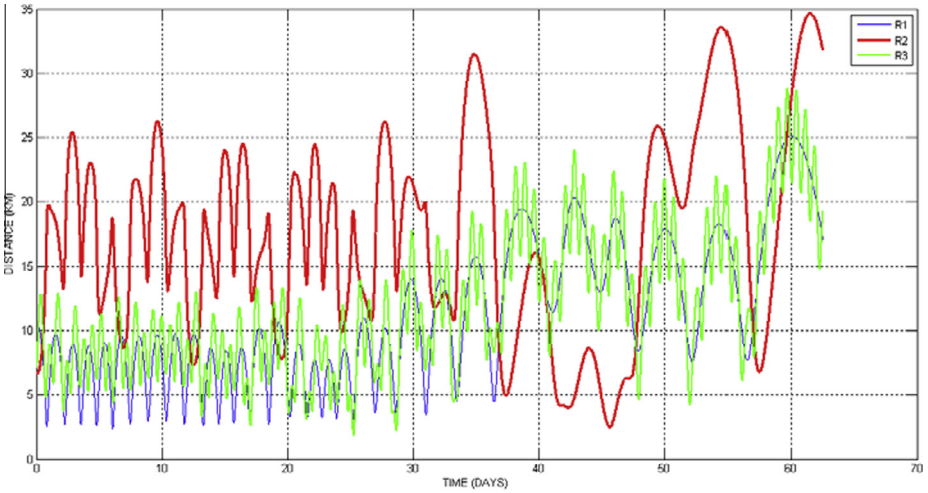

Fig. 9c. Distances of the spacecraft as a function of time from Alpha (blue), Beta (red) and Gamma (green) when there is no radiation pressure for orbit 31. (For interpretation of the references to color in this figure legend, the reader is referred to the web version of this article.)

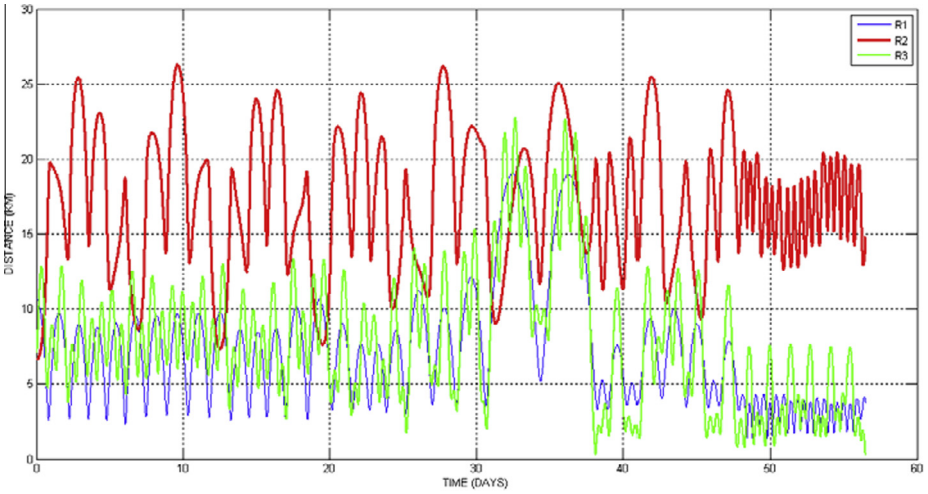

Fig. 9d. Distances of the spacecraft as a function of time from Alpha (blue), Beta (red) and Gamma (green) when there is radiation pressure and the asteroid is at the periapsis for orbit 31. (For interpretation of the references to color in this figure legend, the reader is referred to the web version of this article.)

radiation pressure is neglected, the spacecraft stays 2.25 days near Alpha, 2.80 days near Beta and 3.45 days near Gamma. If the radiation pressure is considered and the asteroid is at the apoapsis of its trajectory around the Sun, those times will be increased and the spacecraft will stay 6.58 days near Alpha, 4.57 days near Beta and 5.82 days near Gamma. It is a significant increase in the durations of the encounters and this trajectory is one of the best to observe the three bodies. The spacecraft also stays 20.79 days near Alpha, 9.27 days near Beta and 19.11 days near Gamma, in the region between 5 and 10 km from the bodies.

Orbit number 31 is shown in Fig. 9, which is an external orbit in resonance 7:2 with Gamma. It is also a trajectory that benefits from the solar radiation pressure. When the radiation pressure is neglected, the spacecraft stays 11.79 days near Alpha, 0.66 days near Beta and 12.38 days near Gamma. If the radiation pressure is considered and the asteroid is at the periapsis of its trajectory around the Sun, those times are changed and the spacecraft stays 5.95 days near Alpha, 5.84 days near Beta and 4.90 days near Gamma. It has a well balanced distribution of durations among the three bodies and this trajectory is one of the best to observe all of them in a single trajectory, in particular if this cycle can be repeated using orbital maneuvers. The spacecraft also stays 20.77 days near Alpha, 10.18 days near Beta and 21.46 days near Gamma, in the region between 5 and 10 km from the bodies.

5. Conclusions

This study was concentrated in searching for natural orbits for a spacecraft to visit the triple asteroid $2001SN_{263}$, which has the property of maximizing the time spent by the spacecraft near one, two or the three bodies of the system.

To make this study, it was defined and implemented a new mathematical model, not found in the literature, that was called "Precessing Inclined Bi-Elliptical Problem with Radiation Pressure" (PIBEPRP). This model took into account the gravitational forces of the three bodies of the triple system, the flattening of the central body, either directly affecting the trajectory of the spacecraft and indirectly, causing a precession in the orbits of the two smaller bodies of the system and the radiation pressure. The inclination between the orbital planes of the two smaller bodies was also considered by the model.

The initial conditions were obtained such that the osculating orbit at the initial time is resonant with the orbit of one of the satellite bodies of the system, in order to increase the probability of multiple close encounters between the spacecraft and the smaller bodies of the system. A maximum number of revolutions were specified, to avoid long orbital periods for the trajectory, which would not be interesting for practical applications. After those initial conditions were obtained, the trajectories were numerically integrated using the dynamical model and the time that the spacecraft remained close to each of the three bodies were measured and plotted.

The results showed that single natural orbits to explore the three bodies are not common, but some good choices do exist. On the other hand, orbits that are very good for the exploration of Alpha and Gamma are easily found, as well as orbits that stay a long time around Beta. These results are interesting, because a combination of the solutions found here may be useful for the mission. The spacecraft can be placed in one of the suitable orbits for the exploration of Alpha and Gamma and then be transferred to an ideal orbit for the exploration of Beta. There are several options for combinations of this type and a final decision depends on the technical details of the mission, like the available fuel and the exact distances required for the observation of each body.

The effects of the radiation pressure depended largely on the particular trajectory. There were several situations where the spacecraft stays longer near the bodies when the radiation pressure was considered, helping to observe the bodies. In some other cases those durations were reduced. In some conditions there was no modification in the results, usually because the spacecraft stays longer times near the bodies and the gravity fields dominate the motion of the spacecraft.

Acknowledgements

The authors wish to express their appreciation for the support provided by grants # 473387/2012-3, 473164/2013-2 and 304700/2009-6 from the National Council for Scientific and Technological Development (CNPq); grants # 2011/08171-3, 2011/13101-4, 2014/06688-7 and 2012/21023-6 from São Paulo Research Foundation (FAPESP) and the financial support from the National Council for the Improvement of Higher Education (CAPES).

References

Araújo, R.A.N., Winter, O.C., Prado, A.F.B.A., Sukhanov, A., 2012. Stability regions around the components of the triple system 2001SN263. Mon. Not. R. Astron. Soc. 423 (4), 3058–3073. http://dx.doi.org/10.1111/j.1365-2966.2012.21101.x.

Bartczakk, P., Breiter, S., Jusiel, P., 2006. Ellipsoids, material points and material segments. Celest. Mech. Dyn. Astron. 96 (1), 31–48. http://dx.doi.org/10.1007/s10569-006-9017-x.

Becker, T.M., Nolan, M., Howell, E., Magri, C., 2009. Physical modeling of triple Near-Earth Asteroid 153591 (2001SN263). Bull. Am. Astron. Soc. 41, 190.

Bellerose, J., Scheeres, D.J., 2008. Restricted full three-body problem: application to binary system 1999 KW4. J. Guidance Control Dyn. 31 (1), 162–171. http://dx.doi.org/10.2514/1.30937.

Belton, M.J.S., Veverka, J., Thomas, P., Helfenstein, P., Simonelli, D., Chapman, C., Davies, M.E., Greley, R., Greenberg, R., Head, R., Murchie, S., Klaasen, K., Johnson, T.V., Mcewen, A., Morrison, D., Neukum, G., Fanale, F., Anger, C., Carr, M., Pilcher, C., 1992. Galileo Encounter with 951 Gaspra: first pictures of an asteroid. Sci., New Ser. 257 (5077), 1647–1652. http://dx.doi.org/10.1126/science.257.5077.1647.

Belton, M.J.S., Chapman, C., Klaasen, K., Harch, A.P., Thomas, P., Veverka, J., Mcewen, A., Pappalardo, R.T., 1996. Galileo's Encounter with 243 Ida: overview of the imaging experiment. Icarus 120 (0032), 1–19. http://dx.doi.org/10.1006/icar.1996.0032.

Broschart, S.B., Scheeres, D.J., 2005. Control of hovering spacecraft near small bodies: application to asteroid 25143 Itokawa". J. Guidance Control Dyn. 28 (2), 343–354. http://dx.doi.org/10.2514/1.3890.

Broucke, R.A., 1988. The celestial mechanics of gravity assist. AIAA paper 88–4220. In: AIAA/AAS Astrodynamics Conference, Minneapolis, MN, 15–17.

Brum, A.G.V., Hetem, A., Rego, I.S., Francisco, C.P.F., Fenili, A., Madeira, F., Cruz, F.C., Assafin, M., 2011. Preliminary development plan of the ALR, the laser rangefinder for the Aster deep space mission to the 2001 SN263 asteroid. J. Aerosp. Tehchnol. Manage. 3 (3), 331–338. http://dx.doi.org/10.5028/jatm.2011.03033611.

Byram, S.M., Scheeres, D.J., 2009. Stability of sun-synchronous orbits in the vicinity of a comet. J. Guidance Control Dyn. 32 (5), 1550–1559.

Fang, J., Margot, J.L., Brozovic, M., Nolan, M.C., Benner, L.A.M., Taylor, P.A., 2011. Orbits of near-earth asteroid triple 2001SN263 and 1994 CC: properties, origin, and evolution. Astron. J. 141 (5), 141–154. http://dx.doi.org/10.1088/0004-6256/141/5/154.

Fieseler, P.D., 1988. A method for Solar Sailing in a low Earth Orbit. Acta Astronaut. 43 (9–10), 531–541. http://dx.doi.org/10.1016/S0094-5765(98)00175-1.

Huntress, W., Stetson, D., Farquhar, R., Zimmerman, J., Clarke, B., O'Neil, W., Bourke, R., Foingf, B., 2006. The next steps in exploring deep space – a cosmic study by the IAA. Acta Astronaut. 58, 304–377.

Jones, T., Lee, P., Bellerose, J., Fahnestock, E., Farquhar, R., Gaffey, M., Heldmann, J., 2011. Asteroid system 2001 SN263. The 42nd Lunar and Planetary Science. Lunar and Planetary Institute, The Woodlands, Texas.

Kuga, H.K., Kondapalli, R.R., Carrara, V., 2012. Introdução à Mecânica Orbital. 2. Ed. São José dos Campos: INPE. pp. 67. (sid.inpe.br/mtc-m05/2012/06.28.14.21.24-PUD). Available in: <http://urlib.net/8JMKD3MGPAW/3C76K98>. Acesso em 14 abr. 2015.

Macau, E.E., Winter, O.C., Velho, H.F.C., Sukhanov, A.A., Brum, A.G.V., Ferreira, J.L., Hetem, A., Sandonato, G.M., Sfair, R., 2010. The Aster Mission: Exploring for the First Time a Triple System Asteroid. In: 62nd International Astronautical Congress, Cape Town, IAC-11-B4-2.7.

Masago, B.Y.P.L., 2014. Estudo de órbitas ressonantes no sistema triplo 2001SN263. Dissertion of Master degree (in Portuguese). São José dos Campos, Brasil. INPE

Murray, D.C., Dermott, S.F., 1999. Solar System Dynamics. Cambridge University Press, New York, pp. 591.

Nolan, M.C., Howell, E.S., Benner, L.A.M., Ostro, S.J., Giorgini, J.D., Busch, M.W., Carter, L.M., Anderson, R.F., Magri, C., Campbell, D. B., Margot, J.L., Vervack, R.J., Shepard, M.K., 2008. Arecibo Radar Imaging of 2001SN263: a near-Earth triple asteroid system. In: Asteroid, Comets and Meteors Conference, No. 1405, Baltimore.

Prado, A.F.B.A., 2014a. Mapping orbits around the asteroid $2001SN_{263}$. Adv. Space Res. 53, 877–889. http://dx.doi.org/10.1016/j.asr.2013.12.034.

Prado, A.F.B.A., 2014a. Mapping Swing-By Trajectories in the Triple Asteroid 2001SN263. In: 13th International Conference on Space Operations 2014, Pasadena. 13th International Conference on Space Operations 2014, Pasadena. AIAA 2014–1610. Reston: American Institute of Aeronautics and Astronautics.

Rossi, A., Marzari, F., Farinella, P., 1999. Orbital evolution around irregular bodies. Earth Planets Space 51 (11), 1173–1180.

Scheeres, D.J., 1994. Dynamics about uniformly rotating triaxial ellipsoids: application to asteroids. Icarus 121, 67–87.

Scheeres, D.J., Hu, W., 2001. Secular motion in a 2nd degree and order gravity field with no rotation. Celest. Mech. Dyn. Astron. 79 (3), 183–200. http://dx.doi.org/10.1023/A:1017555005699.

Scheeres, D.J., 2012a. Orbital Motion in Strongly Perturbed Environments. Springer, Berlin, ISBN 978-3-642-03255-4.

Scheeres, D.J., 2012b. Orbit mechanics about asteroids and comets. J. Guidance Control Dyn. 35 (3), 987–997. http://dx.doi.org/10.2514/1.57247.

Scheeres, D.J., 2012c. Orbital mechanics about small bodies. Acta Astronaut. 72, 1–14. http://dx.doi.org/10.1016/j.actaastro.2011.10.021.

Sukhanov, A.A., Velho, H.F.C., Macau, E.E., Winter, O.C., 2010. The aster project: flight to a near-earth asteroid. Cosm. Res. 48 (5), 443–450. http://dx.doi.org/10.1134/S0010952510050114.

Surovik, D.A., Scheeres, D.J., 2014. Autonomous maneuver planning at small bodies via mission objective reachability analysis. In: AIAA/AAS Astrodynamics Specialist Conference. doi: http://dx.doi.org/10.2514/6.2014-4147. .

Venditti, F., Prado, A.F.B.A., 2014. Mapping orbits regarding perturbations due to the gravitational field of a cube. Math. Prob. Eng. http://dx.doi.org/10.1155/2015/493903.

Veverka, J., Farquhar, B., Robinson, M., Thomas, P., Murchie, S., Harch, A., Antreasian, P.G., Chesley, S.R., Miller, J.K., Owen, W.M., Willians, B.G., Yeomans, D., Dunham, D., Heyler, G., Holdridge, M., Nelson, R.L., Whittenburg, K.E., Ray, J.C., Carcich, B., Cheng, A., Chapman, C., Bell, J.F., Bell, M., Bussey, B., Clark, B., Domingue, D., Gaffey, M.J., Hawkins, E., Izenberg, N., Joseph, J., Kirk, R., Lucey, P., Malin, M., McFadden, L., Merline, W.J., Peterson, C., Prockter, L., Warren, J., Wllnitz, D., 2001. The landing of the Near - Shoemaker spacecraft on asteroid 433 Eros. Nature 413 (6854), 390–393. http://dx.doi.org/10.1038/35096507.

Werner, R.A., 1994. The gravitational potential of a homogeneous polyhedron or don't cut corners. Celest. Mech. Dyn. Astron. 59 (3), 253–278. http://dx.doi.org/10.1007/BF00692875.

Yoshikawa, M., Fujiwara, A., Kawaguchi, J., 2007. Hayabusa and its adventure around the tiny asteroid Itokawa. Proc. Int. Astron. Union 2, 323–324. http://dx.doi.org/10.1017/S174392130701085X.